مؤتمر الأزهر الهندسي الدولي الحادي عشر

AL-AZHAR ENGINEERING
ELEVENTH INTERNATIONAL CONFERENCE
December 21 - 23, 2010

Code : C 26

ON THE LONG-TERM PERFORMANCE OF SUBSURFACE STRUCTURES

Mohamed A. Meguid , Cheehan Leung and Hoang K. Dang
Civil Engineering and Applied Mechanics, McGill University, Montreal, Quebec, Canada

ABSTRACT
Subsurface infrastructures in larg cities are more than 50 years old and billions of dollars are spent every year across the world to repair deteriorated tunnels, buried pipes and other underground facilities. Extensive research has been done in the past few decades to investigate the performance of these structures in their initial configuration over their service life. Actual failure often involves changes in soil and structural components and their interaction. The mechanics of soil weakening in the vicinity of a subsurface structure is a challenging soil-structure interaction problem that involves particle movement and lining separation from the supporting ground. In this study, experimental and numerical investigations are conducted to examine the effect of soil weakening and local support loss on the contact pressure distribution and internal forces in a tunnel lining. A testing facility was designed and built to measure the changes in pressure due to an induced local separation between the lining and the surrounding soil. Significant increase in contact pressure was measured at the boundaries of the separation zone. The results of a three-dimensional Discrete-Finite element analysis indicated a drastic increase in the bending moment in a tunnel lining experiencing particle loss and soil weakening near its crown. Efforts have to be made to detect and control soil weakening and support loss near existing subsurface structures.

Keywords: soil-structure interaction, subsurface structures, numerical analysis, physical modeling, discrete-finite element analysis.

1. INTRODUCTION
Local support loss may develop around underground tunnels and other subsurface structures (pipes, vertical shafts, etc.) due to several reasons including improper grouting and erosion of the supporting soils. This can lead to re-distribution of the earth pressures acting on the tunnel and changes the internal forces in the lining structure. Several case histories involving lining damage due to soil erosion have been reported in the literature. Among the recent cases, two sewer tunnels and one water tunnel in the U.S. in addition to a transportation tunnel in Japan (ITA, 1991). In all cases, tunnels were built in silty or sandy soils and experienced a loss of soil support

around the springlines and invert of the tunnel lining. It has been observed that support loss at the tunnel invert causes differential settlement which leads to circumferential cracking whereas support loss at the sides causes ovalisation and longitudinal cracking of the lining. Talesnick and Baker (1999) reported the failure of a large diameter (1.2 m) composite pipe due to the development of a 200 mm void beneath the invert that extended 300 m along the pipe. These examples illustrate the possible disastrous consequences of the support loss around existing buried structures.

Very few studies have been devoted to investigate the effect of soil weakening and void formation around tunnels and buried pipes on the long-term performance of these structures. Tan and Moore (2007) investigated numerically the effect of void formation on the performance of buried rigid pipes. The influence of both the void size and location (e.g. springline and invert) on the stresses and bending moments developing in the pipe wall was investigated. Results of an elastic model showed that the presence of a void at the springline leads to an increase in the extreme fiber stresses and the bending moments at all critical locations: crown, springlines and invert. The rate of increase is controlled by the growth of the void in contact with the rigid pipe. Meguid and Dang (2009) conducted a numerical study on the effect of erosion void development around an existing tunnel on the circumferential stresses in the tunnel lining. A series of elasto-plastic finite element analysis was carried to investigate the effect of different parameters (e.g., flexibility ratio, coefficient of earth pressure at rest and void size) on thrust forces and bending moments in the lining. When the void was located at the springline, bending moment significantly increased. Similar results were reported for the thrust forces under the same conditions regardless of the flexibility ratio. The presence of erosion void at the lining invert was found to reduce the bending moments causing reversal in the sign of the moment as the void size increased.

The above studies contributed to the understanding of how the presence of voids would affect the performance of an existing pipe constructed using either conventional methods or tunneling techniques. However, experimental studies are needed to confirm the above findings and provide additional information about the effect of soil weakening and local support loss on the earth pressure distribution acting on a buried structure. The objective of this study is to experimentally investigate the effects of local contact loss around an existing tunnel on the earth pressure distribution on the tunnel lining. The experimental study is briefly described and the measured earth pressure results are summarized and compared with the initial earth pressure values. A numerical model that has been developed using the Discrete-Finite Element (DE-FE) approach is then described and preliminary results are presented.

2. EXPERIMENTAL STUDY

A testing facility has been designed and built such that the entire model was contained in a rigid steel tank. As illustrated in Fig. 1, the tank is approximately 1410 mm wide, 1270 mm high and 300 mm thick with a 12 mm plexiglass face. Both the front and rear sides were reinforced using three 100 mm HSS sections. The internal steel sides of the tank were painted and lined with plastic sheets to reduce friction between the sand and the sides of the tank. On the front and rear sides, a hole of 152 mm in diameter was drilled. The hole size was chosen to be larger than the outer diameter of the tunnel to ensure that the tunnel rests directly on the sand. The location of the opening was selected to minimize the influence of the tank rigid boundaries on the measured earth pressure and to ensure sufficient overburden pressure over the tunnel with cover to diameter (C/D) ratio of 2. This was achieved by placing the lateral boundaries at a distance of

approximately four times the tunnel diameter (4.2D) measured from its circumference. The tank rigid base was located at a distance of 2.2D below the tunnel invert to represent the case of a tunnel installed in soft ground overlying bedrock.

One of the challenges of the experimental setup was to develop a suitable mechanism to simulate the local contact loss between the tunnel wall and the surrounding medium while recording the corresponding earth pressure changes around the tunnel. This was achieved by designing and machining a segmented lining composed of six curved segments sliced from a cold drawn steel pipe (114 mm in diameter and 610 mm in length) and six aluminum strips. To hold the different circular sectors of the pipe, six stainless steel U-shape grooved pieces were used. Figure 2 shows parts of the model tunnel as well as its inner mechanics. Under full expansion condition, the tunnel outer diameter is 150 mm.

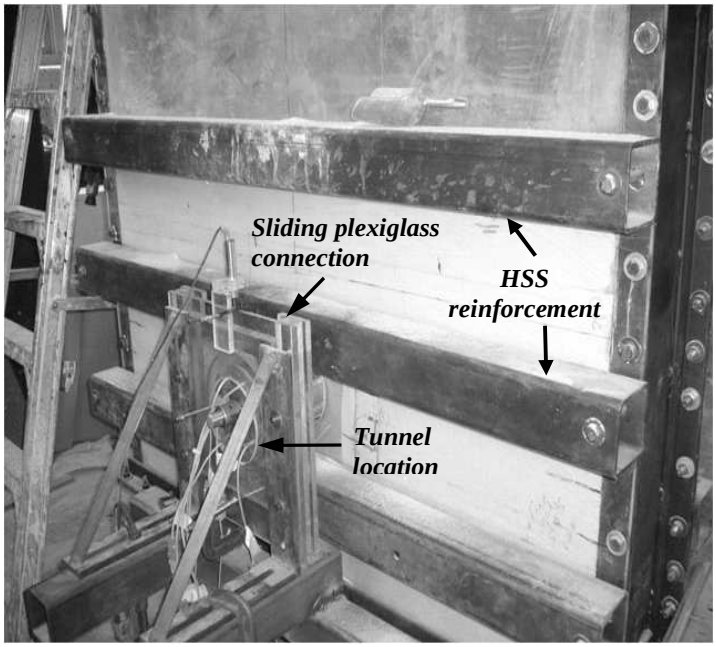

Fig . 1. Test setup

To simulate the local contact loss, a small retractable window was installed on one of the thick lining plates. This small window measured 0.4 inch (10 mm) by 10 inches (254 mm). The retraction method of the window was a miniature version of the tunnel contraction mechanism, the difference being that in the case of the window; only one small plate needs be retracted. Otherwise the action included two small threaded rods of opposing directions that were connected together at the center of the plate by a custom made coupling nut. To move the window, a threaded rod was turned, causing the hinges to move towards the coupling nut and therefore the window moves inward. The window was calibrated to retract exactly 1.5 mm per full (360°) rotation with a maximum retraction of 3.5 mm. The tunnel was designed so that the window could be positioned at the springline, invert and at haunch.

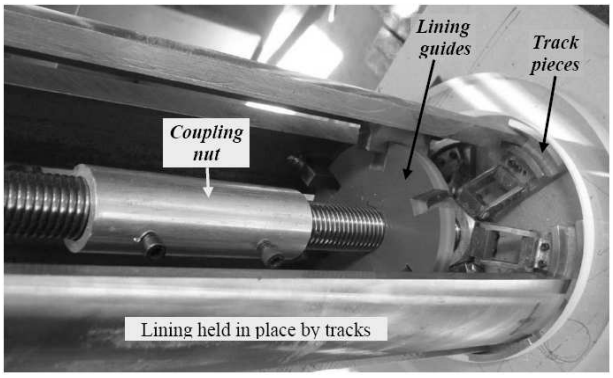

Fig . 2. The mechanically adjustable tunnel

Contact pressure measurement: To measure the earth pressure distribution, the lining was instrumented with eight sensors connected to a data acquisition system. Four of the sensors have maximum capacity of 1200 g with accuracy of ± 0.02% while the remaining ones have maximum capacity of 250 g with accuracy of ± 0.05%. All sensors were mounted inside the pipe with only the sensing area installed flush with the pipe circumference and exposed to the soil. It should be noted that the sizes of the different sensors were chosen such that all sensors fit inside the model tunnel and at the same time provide the accuracy needed for the expected changes in soil pressure. Quartz Industrial 7030 sand was used as the backfill material. Soil characterization and direct shear tests were performed on several randomly selected samples. A summary of the sand properties is provided in Table 1.

Table 1: Soil Properties

Property	Value
Maximum dry unit weight (γ_{max})	15.7 (kN/m^3)
Minimum dry unit weight (γ_{min})	14.1 (kN/m^3)
Experimental dry unit weight (γ_d)	15 (kN/m^3)
Internal friction angle (ϕ)	39°

To ensure the loads cells measure the correct pressures, the entire tunnel model was subjected to a hydrostatic pressure and the readings were recorded and compared with the expected pressure values. Results indicate a linearly increasing pressure with depth. At a depth of 0.9 m below water surface, the maximum hydrostatic pressure was found to be 8.6 kPa which is consistent with the expected value of $\gamma_w h_w$ = 9.81 x 0.9 = 8.8 kPa. The procedure consisted of installing the tunnel under contracted condition (144 mm OD) in the tank. As the tunnel crosses the tank face, two rubber membranes having 150 mm diameter hole were slipped from inside the tank. The tunnel was expanded to its maximum diameter (150 mm) and its horizontal position was checked. Two machined plexiglass connections were installed at the extremities of the pipe to facilitate free sliding in the vertical direction (See Fig. 1). The external plexiglass connections attached to the tunnel were lifted and clamped to prevent the tunnel from resting directly on the rigid boundaries of the tank. To maintain the horizontal position of the tunnel while the test is running,

two vertical LVDTs were attached to the plexiglass connections and connected to the data acquisition system.

Procedure: A testing procedure was developed in order to ensure consistent initial conditions (i.e. sand density) throughout the conducted experiments. From the tank base up to the tunnel invert, the soil was rained and tamped in three layers 100 mm in height. At this stage, the sensors were switched on to record the earth pressure. Another layer of sand was then added to completely cover the tunnel. The remaining sand required to reach the height of 2D above the crown was placed with no tamping. The clamps holding the tunnel were removed simultaneously allowing it to slide vertically and rest on the bedding sand layer. The horizontal position of the tunnel was re-checked using the recorded readings of the vertical LVDTs attached to the plexiglass connections. Once the initial conditions were established, the next step was to contract the tunnel to induce radial soil movement. The contraction was carefully monitored by LVDTs until a decrease of 2 mm in diameter was reached. Retracting the window to simulate a local support loss was the last step of the test. Since the window could retract up to 3 mm, this action was split into two parts each representing a movement of 1.4 mm away from the sand. After each retraction, the sensor readings were recorded and the test completed. The experiments were conducted and repeated three times for each window position (springline, invert and haunch) with a total of nine experiments performed in this study. The developed testing procedure described above was strictly followed for each test to ensure consistent initial conditions. Selected results for two of the window positions (springline and invert) are presented in Figures 3 and 4 and discussed below.

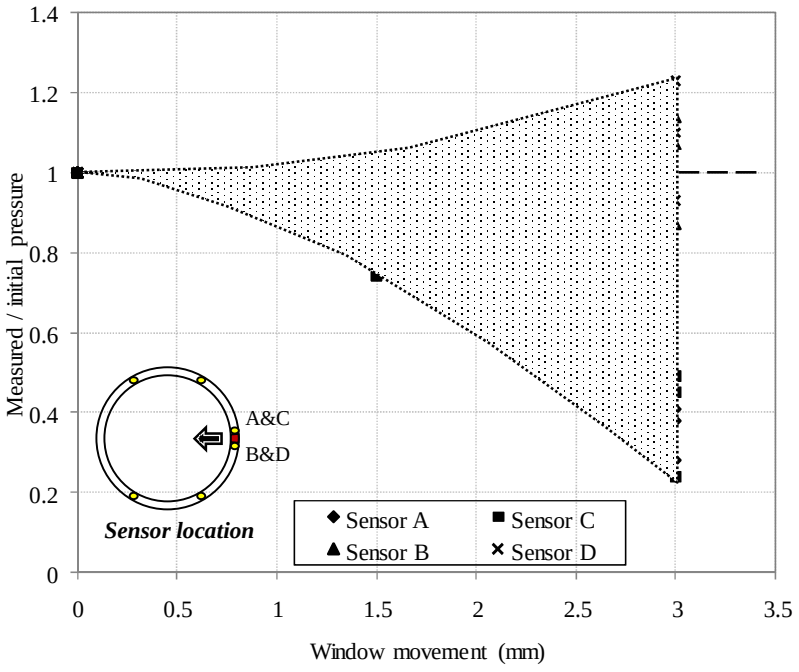

Fig . 3. Measured changes in contact pressure around the retracted window at the springline

Results: Figure 3 shows the measured changes in contact pressure (from the three conducted tests) as recorded by the sensors located in the vicinity of the retractable window versus the

window movement. The pressure is normalized with respect to the initial condition. When positioned at the springline, the retraction of the window produced different pressure readings in the sensors located immediately above and below the window. In sensors A and C located above the window, the pressure gradually decreased as the window was retracted whereas the pressure reading in sensors B and D located below the window slightly increased. The maximum decrease in pressure of the upper sensors reached about 75% of the initial pressure when a retraction of 3 mm was induced. This behaviour can be explained by the soil movement from the area above the window into the created void leading to a release in contact pressure in the close vicinity of the upper sensors.

Figure 4 shows the pressure changes measured in the three conducted tests when the retracted window was located at the tunnel invert. All four sensors measured an increase in pressure with the retraction of the window. For a retraction of 1.5 mm, the maximum pressure increase reached about 7% of the initial pressure and continued to increase to about 23% of the initial pressure when the retraction reached 3 mm.

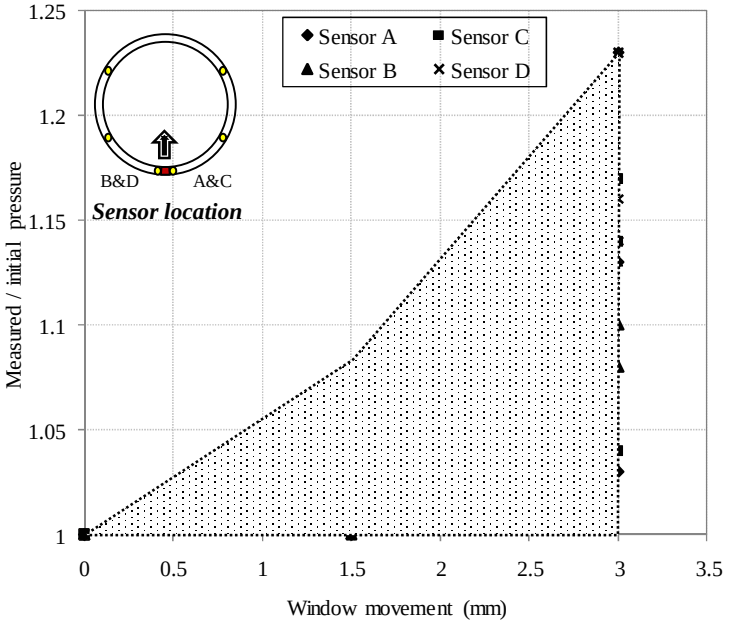

Fig . 4. Measured changes in contact pressure around the retracted window at the invert

3. NUMERICAL MODEL

To understand the impact of soil weakening on the stress changes in an existing structure, a combined Discrete-Finite element model has been used. The domain involving the large displacement is modeled using the discrete elements whereas the rest of the domain is modeled using finite elements. The adopted packing scheme is based on the algorithm of Dang and Meguid (2010a) as illustrated in Figure 5.

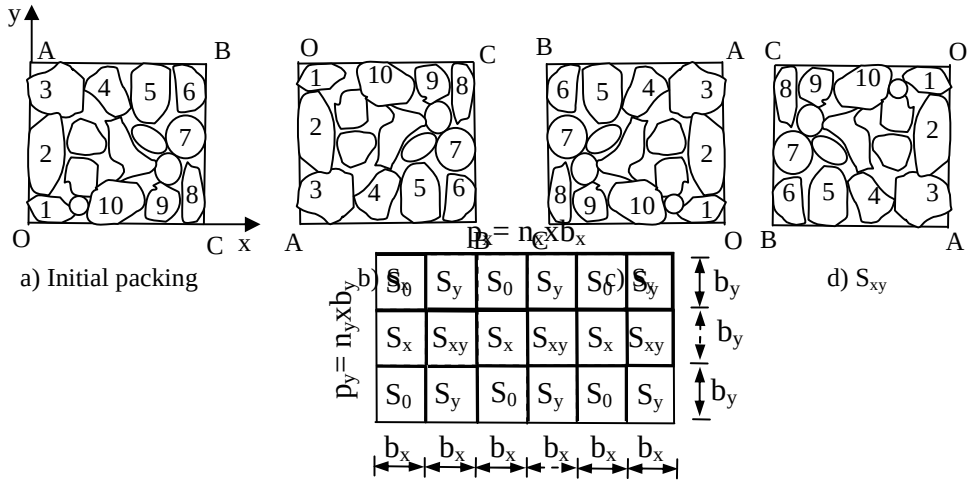

Fig . 5. The flipping scheme of the discrete element packing

To generate a final packing with dimensions of p_x and p_y in the x and y directions, respectively, the packing space is divided into n_x x n_y domains. An initial packing S_0 (b_x x b_y) is first generated to satisfy a target properties and then cloned repeatedly to obtain a final packing with similar properties (grain size distribution, porosity, mean coordination number and fabric tensors). As the structure of the packing is mainly supported by the force chains, it is necessary to maintain the force chains in each initial packing after the assembly. This is achieved by flipping the initial packing such that all particles (initially in contact with the walls) become in contact with other particles in the final packing. As shown in Figure 5, sample S_x is obtained by flipping S_0 around the x axis. Similarly, S_y is obtained by flipping S_0 around the y axis. Finally, S_{xy} is obtained by flipping S_x around the y axis (or flipping S_y around the x axis). The samples S_0, S_x, S_y and S_{xy} are then placed into the space of the final packing. After filling up the final domain, the simulation continued until the final packing satisfies the stability condition.

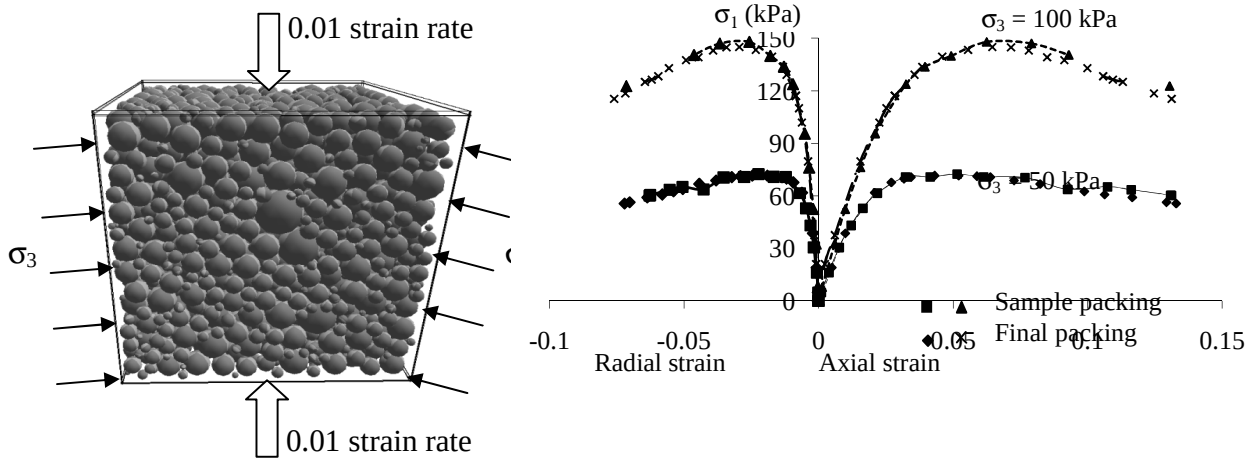

Fig . 6. Triaxial test

Triaxial tests are carried out on a sample generated using the above packing technique as shown in Figure 6. Boundaries are moved at a strain rate of 0.01. This value is chosen so that the unbalanced force is significantly small compared to the contact force, i.e. the system is always

close to equilibrium. The sample is firstly compressed isotropically using an all-around confining pressure. Two different values of confining stresses are adopted, namely 50 kPa and 100 kPa, in the analysis. After the stability condition is reached, additional 0.01 strain rate is applied to the top wall while the lateral confining pressure is kept constant. The reaction stresses are then calculated from the contact forces acting on the walls. During the simulation, gravity field is set to zero.

Figure 6 illustrates the stress strain behaviour of the sample and final packing under confining stresses of 50 kPa and 100 kPa, respectively. The initial stiffness generally increased with increasing the confining stress. The peak strengths are identical for both the sample and final packing regardless of the applied confining stresses. This is attributed to the insignificant difference between the sample and the final packing structures (coordination numbers, porosities and fabric tensors).

Combined DE-FE Method: A combined discrete-finite element method applicable for nonlinear large deformation problems in three-dimensional space has been developed. The domain involving the large displacement is modeled using discrete elements whereas the rest of the domain is modeled using finite elements. Forces acting on discrete and finite elements are restrained by interface elements located at the boundary of the two domains. The adaptive dynamic relaxation algorithm developed by Dang and Meguid (2010b) was used in the FE formulation whereas the technique described above was used in the discrete element. The central-difference time integration scheme was adopted for both FE and DE sub domains. Details of the formulation and calibration of the developed method are provided elsewhere (Dang and Meguid, 2010c).

Tunnel analysis in Mohr-Coulomb material: The analyzed tunnel has a circular cross section with a diameter of 4 m and constructed at a depth of 10 m below the ground surface as shown in Figure 7. The lining is modeled using Belytschko-Tsay shell element elements (Belytschko *et al.*, 1992), whereas the soil is modeled using 8-noded hexahedron elements with hourglass control. The soil volume in the vicinity of the tunnel is modelled using spheres (between Y = 8 m to Y = 12 m). In order to reduce the amount of computation, the spheres located between Z = - 10 m and - 4 m have radii that follow a uniform distribution around a mean value of 0.065 m whereas the spheres located between Z = - 4 m and 0 m have radii that follow a uniform distribution around a mean value of 0.14 m. Following the generation of the initial condition, the soil elements inside the tunnel perimeter were deactivated and a predetermined inward radial displacement was imposed (gap closure) before the final lining is installed. After all nodes have moved to the tunnel perimeter, the lining is activated and the simulation continued until the stability condition is reached.

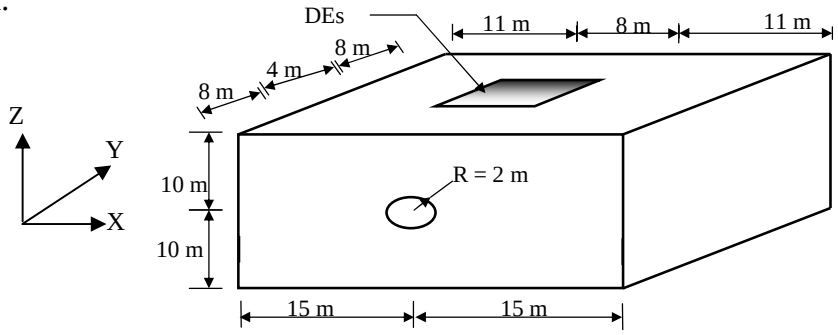

Fig . 7. Geometry of the large scale tunnelling problem

The DE-FE results have been validated by comparing the calculated initial thrust forces and bending moments in the tunnel lining with those obtained using the commercial finite element software Plaxis 3D Tunnel (Brinkgreve and Vermeer, 1998). The calculated moments at the springline and invert were found to be -14.5 kN.m and 12.4 kN.m, respectively. These values are in good agreement with Plaxis analysis (-14.3 kN.m and 13.8 kN.m) at the same examined locations. This confirms that the discrete elements are well representing the soil properties and the interface algorithm is accurate. Figure 8 shows the bending moment distribution along the tunnel lining under the initial conditions.

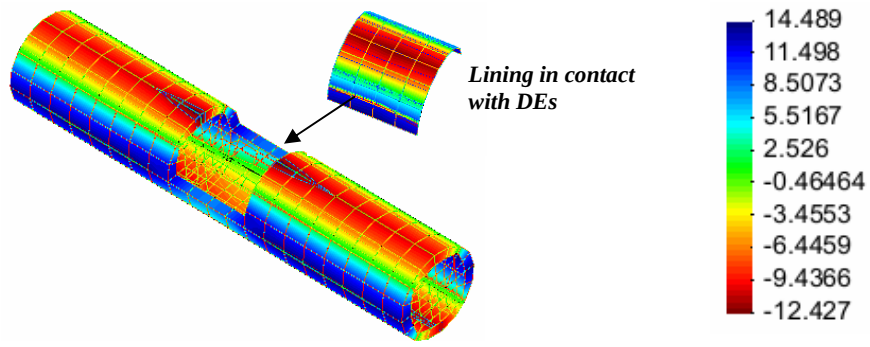

Fig . 8. Bending moment distribution in the tunnel lining

A zone of weakened soil was introduced near the tunnel crown by removing DE particles within a predefined spherical area. The center of the weakened zone was located at X = 15 m, Y = -10 m and Z = 10 m (see the problem geometry in Figure 5). The size of the weakened zone was incrementally increased in four steps by increasing the diameter from 0.5 m to 2 m.

Preliminary results confirmed the experimental findings and revealed a significant increase in bending moments in the lining when the weakened zone was introduced. It was also found that as the size of the weakened zone increased the bending moment rapidly increased particularly at the zone boundaries and reached about 150% of the initial values when the diameter of the weakened zone reached 2 m. Less profound changes in the thrust forces were calculated with the introduction of the weakened zone. The increase in thrust forces reached a maximum value of 50% of the initial forces.

It is clear that ensuring full contact between the lining and surrounding ground is critical for the long-term performance of existing tunnels and can minimize lining distresses and costly rehabilitation. Further investigation into the role of soil properties and the detailed modeling of the segmented lining is recommended for future research.

4. SUMMARY AND CONCLUSIONS

Experimental investigations have been conducted to examine the role of local contact loss between a tunnel and the supporting soil on the earth pressure distribution and on the lining. A mechanically adjustable lining has been designed to facilitate the simulation of the soil movement around the lining during construction. A retractable window positioned at three different positions (springline, invert and haunch) has been used to represent the contact separation. Pressure cells installed in the close vicinity of the window were used to measure the

changes in pressure due to the progressive retraction of the window. The introduction of the local contact loss at the springline caused pressure increase of about 25% of the initial values immediately below the separation zone and pressure decrease of about 75% right above the springline.

DE-FE analyses were conducted to evaluate the role of soil weakening in the vicinity an existing tunnel on the internal forces in the tunnel lining. Significant increase in bending moment was calculated in the immediate vicinity of the weakened zone. Efforts have to be made to detect and control the size of the weakened soil zones as soon as they develop around subsurface structures.

ACKNOWLEDGEMENT

This research is supported by the Natural Sciences and Engineering Research Council of Canada (NSERC) under grant number 311971-06. The assistance of Mr. John Bartczak in building the tunnel apparatus and conducting the experiments is really appreciated.

REFERENCES

Belytschko, T. “Advances in one-point quadrature shell elements”. Computer methods in applied mechanics and engineering, **1992**, 96(1), 93.

Dang, H. K., and Meguid, M. A. “Algorithm to Generate a Discrete Element Specimen with Predefined Properties”. International Journal of Geomechanics, **2010a**, 10(2), 85.

Dang, H. K., and Meguid, M. A. “Evaluating the performance of an explicit dynamic relaxation technique in analyzing non-linear geotechnical engineering problems”. Computers and Geotechnics, **2010b**, 37(1-2), 125.

Dang, H. K., and Meguid, M. A. “A combined DE-FE method for nonlinear geotechnical engineering problems”. International Journal of Geomechanics, **2010c**, (submitted).

ITA. “Report on the Damaging Effects of Water on Tunnels During Their Working Life”. Tunnelling and Underground Space Technology, **1991**, 6 (1), 11 – 76.

Meguid, M.A.,and Dang, H.K. “The effect of erosion voids on existing tunnel linings”. Tunnelling and Underground Space Technology, **2009**, 24 (3), 278 – 286.

Talesnick, M., Baker, R. “Investigation of the Failure of a Concrete-Lined Steel Pipe”. Geotechnical and Geological Engineering, **1999**, 17, 99 – 121.

Tan, Z.,and Moore, I.D. “Effect of Backfill Erosion on Moments in Buried Rigid Pipes”. Transportation Research Board Annual Conference, **2007**, Washington D.C. January, 29.